Frequency-domain Computation of Inflow Broadband Noise Due to Interaction of a Rectilinear Cascade of Flat Plates with Incident Turbulence

Dingbing Wei(1), Cheolung Cheong (1)

(1) School of Mechanical Engineering, Pusan National University, Busan, Korea.

PACS: 43.28.Ra

ABSTRACT

This paper deals with the broadband noise due to the interaction between convected turbulent gusts and a rectilinear cascade of flat plates bounded by two parallel walls. An analytic formulation for the acoustic power spectrum due to this turbulence-cascade interaction is derived, which can be used to assess the effects of the span-wise wavenumber components of ingesting turbulent gust on the overall acoustic power spectrum. This three-dimensional theory is deduced based on the two-dimensional theory of Cheong et al. (2006, 2009). The three-dimensional model is shown to provide a close fit to the measured spectrum of rotor-stator interaction. The predictions using this three-dimensional model are also compared with those using the previous two-dimensional model by Cheong et al. (2006; 2009). Through this comparison, it is found that the contributions to the acoustic power of the span-wise wavenumber components of incident turbulent gust is increased as the frequency augments, which is mainly due to three-dimensional dispersion-relation characteristics of acoustic waves. The formulation is also used to make a parametric study about the effects on the power spectrum of the blade number, stagger angle, gap-chord ratio, and Mach number.

INTRODUCTION

In modern society, aircraft has become a widely-used traffic tool. It is urgent for aero-engine manufacturers to develop quieter products. Among all the noise sources of aero-engine, fan noise is the most significant part which can be further categorized into tonal noise and broadband noise. Fan tonal noise has now been lessen with less blades and lower rotation speed of future Ultra High Bypass Ratio engine-design. Fan broadband noise may be categorized into self noise and inflow noise. Self noise is due to interaction between the turbulence generated in the boundary layer on the blade surface and the trailing edge and may be further divided into five categories based on its generation mechanism [1]. Broadband inflow noise originates from interaction between inflow turbulence with rotors or stators.

Previously, many researches on fan broadband inflow noise have been carried out. Smith [2] has developed the first theory based on classical aerodynamic vortex theory to predict the unsteady blade loading and the acoustic field upstream and downstream of a two-dimensional cascade of flat-plate airfoils perfectly aligned with a uniform mean flow. Whitehead [3] has developed the LINSUB code to calculate the unsteady two-dimensional linearized subsonic flow in a cascade, using the theory developed by Smith. Using the Wiener-Hopf techniques, Glegg [4] has given an analytic expression for the unsteady blade loading, acoustic mode amplitude, and sound power output of a three-dimensional rectilinear cascade of blades with finite chord excited by a three-dimensional vortical gust and investigated the effects of blade sweep and oblique gust arrival angles. Using the similar theory, Hanson and Horan [5] also made a research about the broadband noise due to turbulence/cascade interaction. Later on, Hanson [6] extended the research to investigate the influence of lean and sweep on noise of cascades with turbulence

inflow. Cheong et al. [7] generalized Smith theory to broadband noise, defined the concept of critical frequency, and made a fully investigation on modal acoustic power (MAP). Cheong et al. [8] also made a modal-decomposition analysis to assess the effects of its sub-components on modal acoustic power.

Extending the previous works [7, 8] based on two-dimensional theory, this paper investigates the broadband noise due to the interaction between convected turbulent gusts and a rectilinear cascade of flat plates bounded by two parallel walls. An analytic formulation for the acoustic power spectrum due to this three-dimensional turbulence-cascade interaction is derived. The three-dimensional model is shown to provide a close fit to the measured spectrum of rotor-stator interaction. The predictions using this three-dimensional model are also compared with those using the previous two-dimensional model by Cheong et al. [7, 8]. Through this comparison, it is found that the contributions to the acoustic power of the span-wise wavenumber components of incident turbulent gust is increased as the frequency augments, which is mainly due to three-dimensional dispersion-relation characteristics of acoustic waves. Main contribution of this work is to make clear the effects of the span-wise wavenumber components of ingesting turbulent gust on the overall acoustic power spectrum, which reveals that the number of incident turbulent gust modes directly involved in generating cut-on acoustic waves increases as the frequency increase. Therefore, in the lower frequency range, three-dimensional acoustic power is less than its corresponding two-dimensional one, whereas, as the frequency increase, three-dimensional acoustic power spectrum closely follows those of two-dimension. The formulation is also used to make a parametric study on the effects on the power spectrum of the blade number, stagger angle, gap-chord ratio, and Mach number.

RESPONSE OF RECTLINEAR CASCADE TO INCIDENT GUST

The cascade geometry investigated in this paper and its coordinate systems are shown in Fig.1. A three-dimensional cascade of flat-plate airfoils with stagger angle θ is assumed to be located in a two-dimensional uniform flow moving in the direction parallel to the chord, i.e., with zero incident angle. Homogeneous, isotropic turbulence is assumed to be convected with mean flow as a "frozen gust pattern". In Fig.1, (x_1, x_2, x_3) is the unwrapped duct coordinate system, and (y_1, y_2, y_3) is the cascade-fixed coordinate system.
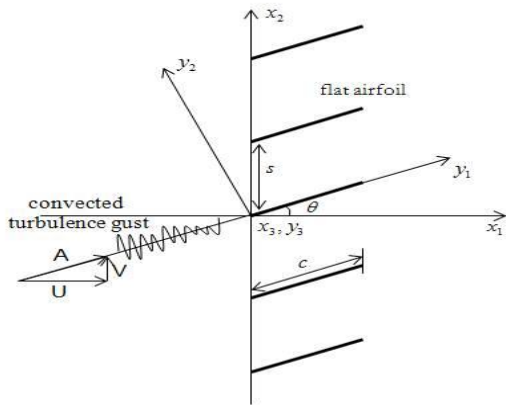
Figure 1. Cascade geometry and convected turbulent gust. x_3 and y_3 coordinates are coming directly out of the page.

The linearised three-dimensional equations of momentum and continuity are

$$\frac{\partial \rho}{\partial t} + U\frac{\partial \rho}{\partial x_1} + V\frac{\partial \rho}{\partial x_2} + W\frac{\partial \rho}{\partial x_3} + \rho_0\left(\frac{\partial u}{\partial x_1} + \frac{\partial v}{\partial x_2} + \frac{\partial w}{\partial x_3}\right) = 0$$

$$\frac{\partial u}{\partial t} + U\frac{\partial u}{\partial x_1} + V\frac{\partial u}{\partial x_2} + W\frac{\partial u}{\partial x_3} + \frac{1}{\rho_0}\frac{\partial p}{\partial x_1} = 0$$

$$\frac{\partial v}{\partial t} + U\frac{\partial v}{\partial x_1} + V\frac{\partial v}{\partial x_2} + W\frac{\partial v}{\partial x_3} + \frac{1}{\rho_0}\frac{\partial p}{\partial x_2} = 0 \quad (1)$$

$$\frac{\partial w}{\partial t} + U\frac{\partial w}{\partial x_1} + V\frac{\partial w}{\partial x_2} + W\frac{\partial w}{\partial x_3} + \frac{1}{\rho_0}\frac{\partial p}{\partial x_3} = 0$$

where U, V and W are the mean velocities in the x_1, x_2 and x_3 directions, respectively; u ,v and w are the corresponding unsteady velocity perturbations; ρ_0 and ρ are the mean and perturbation densities, respectively.

The flow is assumed to be isentropic, so that

$$\left(\frac{\partial p}{\partial \rho}\right)_s = \frac{dp}{d\rho} = a^2 \quad (2)$$

where a is the speed of sound.

For harmonic space and time dependence, the perturbation quantities may be written

$$\begin{vmatrix} u \\ v \\ w \\ p \end{vmatrix} = \begin{vmatrix} \bar{u} \\ \bar{v} \\ \bar{w} \\ \bar{p} \end{vmatrix} \exp i(\omega t + \alpha x_1 + \beta x_2 + \gamma x_3) \quad (3)$$

where $\bar{u}$, $\bar{v}$, $\bar{w}$ and $\bar{p}$ are constant complex amplitudes and α, β and γ are wave numbers. From Eqs. (1), (2) and (3), we can get the condition for a non-trivial solution:

$$(\omega + U\alpha + V\beta + W\gamma)^2$$
$$\times \left[(\omega + U\alpha + V\beta + W\gamma)^2 - a^2(\alpha^2 + \beta^2 + \gamma^2)\right] = 0 \quad (5)$$

Two different physical phenomena are embodied in Eq. (5): acoustic waves and vorticity waves, and these will be considered separately. The acoustic waves satisfy the relations:

$$(\omega + U\alpha + V\beta + W\gamma)^2 - a^2(\alpha^2 + \beta^2 + \gamma^2) = 0 \quad (6)$$

Eq. (6) can be expressed in the form:

$$\alpha = \frac{U(\omega + V\beta + W\gamma) \pm a\sqrt{(\omega + V\beta + W\gamma)^2 - (a^2 - U^2)(\beta^2 + \gamma^2)}}{a^2 - U^2} \quad (7)$$

with the assumption that β and γ are real. The two values of α correspond one to upstream going and the other to downstream going perturbations. Vorticity wave gives the following relation:

$$\left(\omega + U\alpha + V\beta + W\gamma\right)^2 = 0 \quad (8)$$

Eq. (8) can be rearranged for α,

$$\alpha = -\frac{\omega + V\beta + W\gamma}{U} \quad (9)$$

Disturbances of this type propagate without associated pressure fluctuations.

In this paper, the mean flow velocity in x3-direction, W, must be zero to satisfy the boundary condition given in Fig.2. A single wave number component (k_1, k_2, k_3) has a phase angle σ between adjacent blades separated by a gap s given by

$$\sigma = (k_1\sin\theta + k_2\cos\theta)s \quad (10)$$
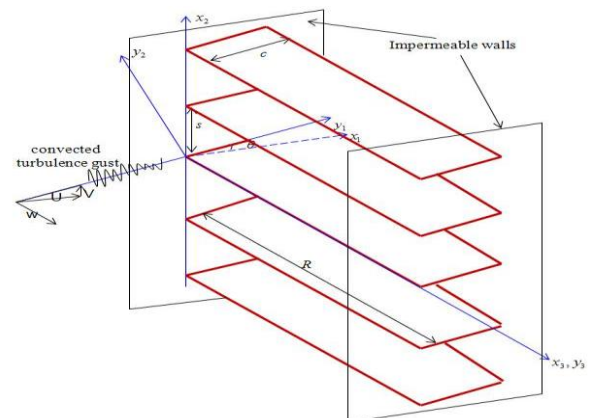
Figure 2. Three-dimensional cascade geometry and the convected turbulent gust.

The phase angle σ between adjacent blades of r-th acoustic wave generated from the cascade due to a single wave number component of vorticity (k_1, k_2, k_3) is of the form $\beta_r s = \sigma - 2\pi r$. So the acoustic circumferential wave number of the r-th acoustic wave is given by

$$\beta_r = \frac{(k_1 \sin\theta + k_2 \cos\theta)s - 2\pi r}{s} \tag{11}$$

Then, the solution for axial wave number can be expressed in terms of β_r, k_3 and ω as:

$$\alpha_r(k_3) = \frac{M_1(\frac{\omega}{a} + M_2\beta_r) \pm \sqrt{(\frac{\omega}{a} + M_1\beta_r)^2 - (1-M_1^2)(\beta_r^2 + k_3^2)}}{1 - M_1^2} \tag{12}$$

Here, the acoustic wavenumber, γ, in the span-wise direction is replaced by the incident vorticity wavenumber, k_3, because the rectilinear cascade is uniform in the x3-direction.

Following to the procedure presented by Smith [2]. For a harmonic gust of the form,

$$w(y_1, y_2, y_3, t) = w_0 e^{i[k_1(y_1 - At) + k_2 y_2 + k_3 y_3]} \tag{13}$$

The acoustic pressure upstream and downstream of the cascade is of the form,

$$p^{\pm}(x_1, x_2, x_3, t) = \rho_0 A w_0 e^{ik_3 x_3} \sum_{r=-\infty}^{\infty} R_r^{\pm}(k_1, k_2) e^{i(k_1 At + \alpha_r^{\pm}(k_3)x_1 + \beta_r x_2)} \tag{14}$$

where R_r is defined as the cascade response function.

EXTENSION TO BROADBAND ACOUSTIC POWER FORMULATION

Assuming that turbulence velocities are much smaller than mean velocities, Taylor's hypothesis can be applied to treat the turbulence as "frozen gust pattern" which is convected with the mean velocities. Then, straightforward extension of the formula for the acoustic pressure for radiation due to an incident three-dimensional sinusoidal vortical gust leads to the expression for broadband acoustic pressure from a cascade subject to the impinging turbulent gust, in the form,

$$p^{\pm}(x_1, x_2, x_3, t) = \rho_0 A \int_{-\infty}^{\infty} \int_{-\infty}^{\infty} \int_{-\infty}^{\infty} \hat{\hat{w}}_D(k_1, k_2, k_3)$$
$$\times e^{ik_3 x_3} \sum_{r=-\infty}^{\infty} R_r^{\pm}(k_1, k_2) e^{i(k_1 At + \alpha_r^{\pm}(k_3)x_1 + \beta_r x_2)} dk_1 \, dk_2 dk_3 \tag{15}$$

where $\hat{\hat{w}}_D(k_1, k_2, k_3)$ is the three dimensional turbulence wave number spectrum of the turbulence velocity evaluated in the moving reference frame. Taking the Fourier transform of Eq. (15) with respect to t, we can transfer the acoustic pressure from time domain to frequency domain in this form,

$$p_T^{\pm}(x_1, x_2, x_3, \omega) = \rho_0 \int_{-\infty}^{\infty} \int_{-\infty}^{\infty} \int_{-\infty}^{\infty} \hat{\hat{w}}_D(k_1, k_2, k_3) \times e^{ik_3 x_3} \sum_{r=-\infty}^{\infty} R_r^{\pm}(k_1, k_2)$$
$$e^{i(\alpha_r^{\pm}(k_3)x_1 + \beta_r x_2)} \times \left\{ \frac{A}{2\pi} \int_{-T}^{T} e^{i(k_1 A + \omega)t} dt \right\} dk_1 dk_2 dk_3 \tag{16}$$

The term within the curly brackets corresponds to a delta-function $\delta(k_1 - K_1)$, where $K_1 = -\omega/A$. Only the component of the turbulence with an axial wave number k_1 equal to K_1 contributes to acoustic pressure. Integration over the axial wave number is therefore trivial and Eq.(16) becomes:

$$\tilde{p}_T^{\pm}(x_1, x_2, x_3, \omega) = \rho_0 \int_{-\infty}^{\infty} \int_{-\infty}^{\infty} \hat{\hat{w}}_D(K_1, k_2, k_3)$$
$$\times e^{ik_3 x_3} \sum_{r=-\infty}^{\infty} R_r^{\pm}(K_1, k_2) e^{i(\alpha_r^{\pm}(k_3)x_1 + \beta_r x_2)} dk_2 dk_3 \tag{17}$$

Substituting Eq.(17) into the momentum equation, we can get acoustic velocities in the axial and gap-wise directions:

$$\tilde{u}_T^{\pm}(x_1, x_2, x_3, \omega) = \rho_0 \int_{-\infty}^{\infty} \int_{-\infty}^{\infty} \hat{\hat{w}}_D(K_1, k_2, k_3) e^{ik_3 x_3}$$
$$\times \sum_{r=-\infty}^{\infty} \frac{-\alpha_r^{\pm}(k_3) R_r^{\pm}(K_1, k_2) e^{i(\alpha_r^{\pm}(k_3)x_1 + \beta_r x_2)}}{\rho_0(\omega + U\alpha_r^{\pm}(k_3) + V\beta_r)} dk_2 dk_3 \tag{18}$$

$$\tilde{v}_T^{\pm}(x_1, x_2, x_3, \omega) = \rho_0 \int_{-\infty}^{\infty} \int_{-\infty}^{\infty} \hat{\hat{w}}_D(K_1, k_2, k_3) e^{ik_3 x_3}$$
$$\times \sum_{r=-\infty}^{\infty} \frac{-\beta_r R_r^{\pm}(K_1, k_2) e^{i(\alpha_r^{\pm}(k_3)x_1 + \beta_r x_2)}}{\rho_0(\omega + U\alpha_r^{\pm}(k_3) + V\beta_r)} dk_2 dk_3 \tag{19}$$

Acoustic power spectrum

To calculate the acoustic power spectrum, the instantaneous acoustic intensity vector for sound propagation in a uniform mean velocity A is required, which formula is given by Goldstein [12]. Substituting Eq.(17)~(19) into Goldstein' equation leads to the formula for the intensity spectrum as:

$$I^{\pm}(x, \omega) = \rho_0 \int_{-\infty}^{\infty} \int_{-\infty}^{\infty} \int_{-\infty}^{\infty} \int_{-\infty}^{\infty} \lim_{T \to \infty} \frac{2\pi}{T} E\left[\hat{\hat{w}}_D(K_1, k_2, k_3) \hat{\hat{w}}_D^*(K_1', k_2', k_3') \right]$$

$$\sum_{r=-\infty}^{\infty} \sum_{r'=-\infty}^{\infty} \text{Re} \left\{ \begin{array}{l} \dfrac{\omega(-\alpha_r^{\pm}(k_3)^* + M_1(\omega/a + M_1 \alpha_r^{\pm}(k_3)^* + M_2\beta_{r'}))}{c_0^2(k + M_1\alpha_r^{\pm}(k_3) + M_2\beta_r)(k + M_1\alpha_r^{\pm}(k_3)^* + M_2\beta_{r'})} \\ \times e^{i(k_3 - k_3')x_3} R_r^{\pm}(K_1, k_2) R_{r'}^{\pm*}(K_1, k_2') \\ \times e^{i((\alpha_r^{\pm}(k_3) - \alpha_{r'}^{\pm}(k_3)^*)x_1 + (\beta_r - \beta_{r'})x_2)} dk_3 dk_3' dk_2 dk_2' \end{array} \right\} \tag{21}$$

Following the procedures presented by Amiet [9], we can get:

$$\lim_{T \to \infty} \frac{2\pi}{T} E\left[\hat{\hat{w}}_D(K_1, k_2, k_3) \hat{\hat{w}}_D^*(K_1, k_2, k_3) \right]$$
$$= A\delta(k_2 - k_2')\delta(k_3 - k_3')\Phi_{ww}(K_1, k_2, k_3) \tag{22}$$

Inserting Eq.(22) into (21) and performing integrations over k_2' and k_3' leads to:

$$I^{\pm}(x, \omega) = \rho_0 M \int_{-\infty}^{\infty} \int_{-\infty}^{\infty} \varphi_{ww}(K_1, k_2, k_3)$$

$$\sum_{r=-\infty}^{\infty} \sum_{r'=-\infty}^{\infty} \text{Re} \left\{ \begin{array}{l} \dfrac{k\left(-\alpha_r^{\pm}(k_3)^* + M_1\left(k + M_1\alpha_{r'}^{\pm}(k_3)^* + M_2\beta_{r'}\right)\right)}{\left(k + M_1\alpha_r^{\pm}(k_3)^* + M_2\beta_r\right)\left(k + M_1\alpha_{r'}^{\pm}(k_3)^* + M_2\beta_{r'}\right)} \\ R_r^{\pm}(K_1, k_2) R_{r'}^{\pm*}(K_1, k_2) \\ e^{i\left((\alpha_r^{\pm}(k_3) - \alpha_{r'}^{\pm}(k_3)^*)x_1 + (\beta_r - \beta_{r'})x_2\right)} dk_2 dk_3 \end{array} \right\} \tag{23}$$

Integrating the above Eq.(23) in the $x_2 - x_3$ plane over an area of $Bs \times R$, we can get the acoustic power. Since the gap-wise direction wave numbers β_r and β_r' are periodic over a distance Bs, this integral is of the form

$$\int_0^R \int_0^{Bs} \exp\left(i(\beta_r - \beta_{r'})x_2\right) dx_2 dx_3 = RBs\delta_{rr'} \tag{24}$$

where the Kroneker delta function $\delta_{rr'}$ enables the r' summation in Eq.(23) to be eliminated. Therefore, the acoustic power spectrum can be expressed as

$$P^{\pm}(\omega) = \rho_0 MRBs \int_{-\infty}^{\infty}\int_{-\infty}^{\infty} \varphi_{ww}(K_1, k_2, k_3)$$
$$\times \sum_{r=-\infty}^{\infty}\left|R_r^{\pm}(K_1, k_2, k_3)\right|^2 \Im_r^{\pm}(k_3)dk_2 dk_3 \qquad (25)$$

where $\Im_r^{\pm}(k_3)$ is non-dimensional acoustic power factor defined as

$$\Im_r^{\pm}(k_3) = \frac{kR_e\left\{-\alpha_r^{\pm}(k_3)^* + M_1\left(K + M_1\alpha_r^{\pm}(k_3)^* + M_2\beta_r\right)\right\}}{\left|K + M_1\alpha_r^{\pm}(k_3)^* + M_2\beta_r\right|^2} \qquad (26)$$

Because of the periodicity of the turbulence spectrum in the x_2 direction, we can use Fourier series instead of the above Fourier integrals. So, the above Fourier integral over k_2 can be converted to Fourier series with the fundamental spatial frequency equal to $2\pi/Bs$. The wave number in the direction are therefore integer multiples of the fundamental spatial frequency and equal to

$$\beta = \frac{2\pi}{BS}m \qquad (27)$$

The turbulence wave numbers k_1 and k_2, defined in the blade-fixed coordinate (y_1, y_2, y_3), can be expressed in the cascade coordinate system (x_1, x_2, x_3), which leads to the following relation,

$$\frac{2\pi}{BS}m = K_1\sin\theta + k_{2,m}\cos\theta \qquad (28)$$

Eq. (28) can be rearranged in the explicit form for $k_{2,m}$:

$$k_{2,m} = \frac{2\pi m}{BS\cos\theta} - K_1\tan\theta \qquad (29)$$

where m is defined as the vortical mode number in the gap-wise direction.

Therefore, integration over k_2 at a constant frequency (or K_1) can be replaced by:

$$\int dk_2 = \frac{2\pi}{Bs\cos\theta}\sum_{m=-\infty}^{\infty} \qquad (30)$$

Similar reasoning can be applied for the k_3 in the x_3 direction. The wave number in the x_3 direction is integer multiples of the fundamental spatial mode j and integration over k_3 can be replaced by:

$$\int dk_3 = \frac{\pi}{R}\sum_{j=-\infty}^{\infty} \qquad (33)$$

Thus, Eq. (25) now turns into:

$$P^{\pm}(\omega) = \frac{2\pi^2\rho_0 M}{R\cos\theta}\sum_{j=-\infty}^{\infty}\sum_{m=-\infty}^{\infty}\varphi_{ww}(K_1, k_{2,m}, k_{3,j})\sum_{r=-\infty}^{\infty}\left|R_r^{\pm}(K_1, k_{2,m})\right|^2 \Im_{r,j}^{\pm}$$
$$(34)$$

where

$$\Im_{r,j}^{\pm} = \frac{kR_e\left\{-\alpha_r^{\pm}(k_{3,j})^* + M_1\left(K + M_1\alpha_r^{\pm}(k_{3,j})^* + M_2\beta_r\right)\right\}}{\left|K + M_1\alpha_r^{\pm}(k_{3,j})^* + M_2\beta_r\right|^2} \qquad (35)$$

Formula (34) shows that the radiated sound power spectrum is due to an infinite number of impinging vortical modes m and j, of which each generates upstream and downstream going acoustic waves. However, Eq. (34) is not efficient when calculating the spectrum of acoustic power because $R_r^{\pm}$ appears inside the three summations over the variables of m, r and j. A transformation of the summation indices can be used to move $R_r^{\pm}$ out from the three summation into a single summation at the expense of moving the turbulence spectrum Φ_{ww} under the three summations. Such an arrangement is advantageous since Φ_{ww} will normally be computed from a simple algebraic expression, whereas $R_r^{\pm}$ requires another infinite summation of the so-called "cascade waves" and the numerical computation of the upwash integral equation in Smith's theory. Since the basic spatial period of the flow is Bs, the acoustic wave number in x_2 direction must satisfy

$$\beta_l = \frac{2\pi}{Bs}l \qquad (36)$$

where l is the acoustic mode in x_2-direction. Inserting Eqs. (29) and (36) into Eq.(11), the m-th vortical wave number may be written in terms of the acoustic mode number l and the cascade scattering index r as

$$m = l + Br \qquad (37)$$

Inserting Eq.(37) into Eq.(29) gives

$$k_{2,l+Br} = \frac{2\pi}{Bs\cos\theta}(l + Br) - K_1\tan\theta \qquad (38)$$

By using Eq.(38), Eq.(34) can be rearranged as:

$$P^{\pm}(\omega) = \frac{2\pi^2\rho_0 M}{R\cos\theta}\sum_{l=-\infty}^{\infty}\left|R_l^{\pm}(K_1, k_{2,\mathrm{mod}(l,B)})\right|^2\sum_{j=-\infty}^{\infty}\sum_{r=-\infty}^{\infty}\Im_{r,j}^{\pm}\phi_{ww}(K_1, k_{2,l+Br}, k_{3,j})$$
$$(39)$$

Turbulence spectra

For simplicity, we just consider the circumstance that the turbulence impinging on the stator is homogeneous and isotropic. Liepmann spectrum $\Phi_{ww}(k_1, k_2, k_3)$ is a very suitable model for wave number PSD:

$$\phi_{ww}(k_1, k_2, k_3) = \frac{2\overline{w}^2\Lambda^3}{\pi^2}\frac{\Lambda^2\left(k_1^2 + k_3^2\right)}{\left(1 + \Lambda^2\left(k_1^2 + k_2^2 + k_3^2\right)\right)^3} \qquad (42)$$

Cut-on condition

Equation (39) defines the acoustic power spectrum due to an infinite summation over the acoustic mode number l. However, if we consider only the propagating wave components in Eq. (39), the infinite summation over l can be reduced to a finite frequency range. In a subsonic flow, $W < a$, propagating acoustic modes correspond to real values of $\alpha_r^{\pm}$, which occur over the range of β_l given by

$$\frac{kM_2 - \sqrt{(1-M_1^2)\left[(M^2-1)\gamma^2 + k^2\right]}}{1-M^2} \le \beta_l$$
$$\le \frac{kM_2 + \sqrt{(1-M_1^2)\left[(M^2-1)\gamma^2 + k^2\right]}}{1-M^2} \tag{43}$$

We use L_{max} and L_{min} to denote the maximum and minimum integers of acoustic mode number l satisfying the upper and lower inequality of Eq.(43). The range of r and j are also selected to ensure the cut-on condition and convergence, respectively. The broadband sound power over the frequency range $\omega_L \le \omega \le \omega_H$ can therefore be integrated as

$$\Pi^\pm = \frac{2\pi^2 \rho_0 M}{\cos\theta} \int_{\omega_L}^{\omega_H} \sum_{l=L_{min}}^{L_{max}} \left| R_l^\pm \left(K_1, k_{2,\mathrm{mod}(l,B)}\right) \right|^2$$
$$\times \sum_{j=-\infty}^{\infty} \sum_{r=-\infty}^{\infty} \mathfrak{I}_{r,j}^\pm \phi_{ww}\left(K_1, k_{2,l+Br}, k_{3,j}\right) d\omega \tag{45}$$

The predicted sound power spectrum are expressed in decibels as a power level (PWL) defined as

$$PWL^\pm = 10\log_{10}\left(\frac{\Pi^\pm}{10^{-12}}\right) \tag{46}$$

COMPARISON WITH EXPERIMENTAL RESULT

Using the 3-D formula derived in the last section, the broadband acoustic power spectrum can be calculated. In this section, a comparison between predicted acoustic power spectrum and a model test data in a wind tunnel at NASA-Lewis is presented in Figure 3. The stator is modeled by the three-dimensional cascade geometry shown in Figure 2, with a mean flow impinge on the tip of the stator with zero incident angle. The parameter data used in this computation is shown in Table 1. Turbulence scale and intensity were adjusted to provide a good match between the predicted data and the experimental result.

Table 1. Parameters used for the acoustic power spectrum prediction

M	B	s/c	θ	$\overline{w^2}/W^2$	Λ/R	R
0.5	45	0.8	30°	4.2×10^{-4}	0.035	0.8
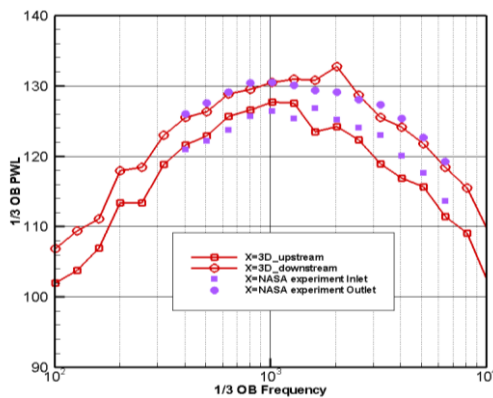
Figure 3. Comparison of acoustic power spectrum between the predictions and experimental result for a scaled model.

Although the turbulence properties are represented simply by the Liepmann model with a single value of turbulence intensity and scale, the agreement between the predicted acoustic power spectrum and the measurement is good, as shown in Figure 3. In addition, the difference between the predicted

upstream and downstream acoustic power spectrum closely matches experimental data.

COMPARISON WITH 2-D RESULT

In Fig. 4, acoustic power spectra predicted using the present three-dimensional model are compared with those using the previous two-dimensional formulation [7, 8]. The parameters used in this calculation followed the baseline case used in the last section, except that the mean square value of turbulence velocity $\overline{w^2}$ was changed to $\overline{w^2}/W^2 = 4\times10^{-4}$. Note that the difference in magnitudes between the three-dimensional and two-dimensional spectra is induced by the difference of incident turbulence velocities: in two-dimensional model, the turbulence spectrum $\Phi_{ww}(k_1, k_2, k_3)$ is integrated over all the range of k_3 modes, while for three-dimensional model, it is only integrated over a finite number of k_3 modes satisfying the boundary condition as given in Eq. (32). Therefore, it is physically meaningless to compare their magnitudes. Instead, variations of spectra according to the frequency are of physical importance. As shown in Figure 4, high-frequency roll-off of the acoustic power spectra predicted using the present model closely follows that of the the two-dimensional model prediction. However, the positive slope of the spectra at lower frequencies, predicted using the present model, is steeper than that of two-dimensional predictions. Based on these observations, it can be inferred that as the frequency increases acoustic power spectrum due to three-dimensional interaction of ingesting turbulence with the rectilinear cascade of flat-plates more resembles that in two-dimension. This result may be explained by the fact that the number of the span-wise wavenumber components of incident turbulent gust involved directly in contributing to the acoustic power is increased as the frequency augments. These characteristics of three-dimensional acoustic field are mainly due to the dispersion-relation properties of three-dimensional acoustic waves: the lowest cut-on frequency increases as the span-wise wavenumber increases, which is quite different from two-dimensional ones . The approach used in the two-dimensional prediction is to start with a three-dimensional turbulence spectrum, integrate over all spanwise wavenumbers, and then apply this reduced spectrum at zero spanwise wavenumber. i.e., all input gusts are in phase along the full vane span This difference characterizes the broadband noise due to the interaction between the turbulence and rectilinear cascade, compared with its corresponding two dimensional one. Important implication of this finding is that the high-frequency approximate expression, proposed by Cheong et al. [7] to effectively predict the acoustic power spectrum due to turbulence-cascade interaction, can be still applied for the prediction of acoustic power due to this three-dimensional interaction.
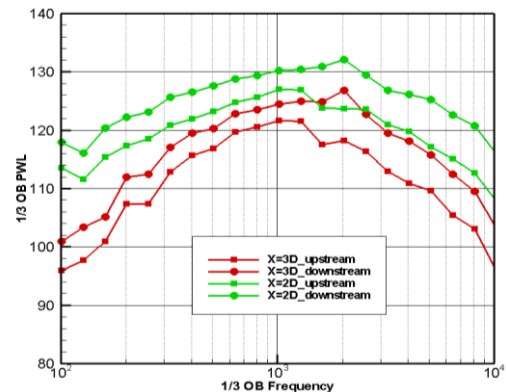
Figure 4. Comparison of the 3-D prediction with the two-dimensional prediction of Cheong et al. [7, 8].

PARAMETRIC STUDY

In this section, we examine the effect of different parameters on the acoustic power spectrum. For the parametric studies shown in this section, a baseline case is chosen to correspond to that used in Sec.V. This parametric study is a useful reference for stator designers.

Figure 5 shows the variation of one-third octave band power levels for $B = 15, 30, 60$. In the high frequency range, approximately $f \geq 1000$ Hz, the acoustic power both upstream and downstream is observed to be proportional to B, same as that observed in the two-dimensional cases of works [7, 8].

(a)

(b)
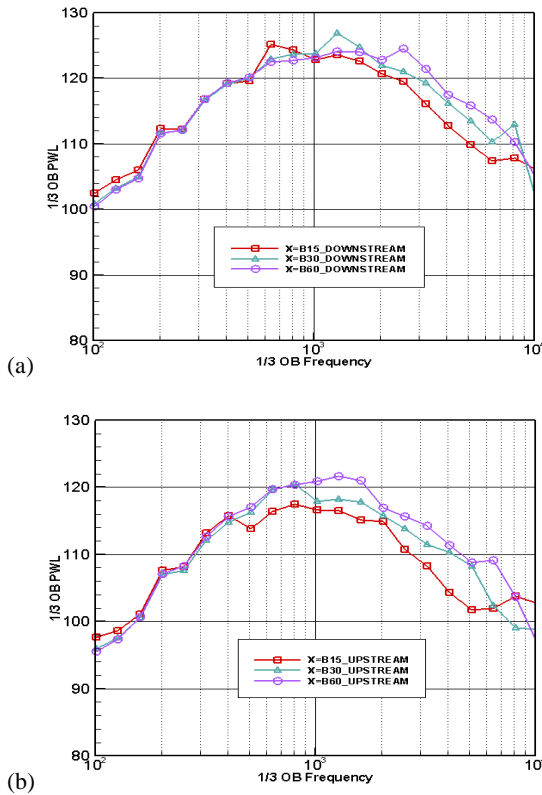
Figure 5. Variation of acoustic power spectrum with blade number, B. (a) upstream and (b) downstream.

Figure 6 shows the power spectrum for the stagger angle of $15°$, $30°$ and $45°$. At the high frequency range, the acoustic power upstream is observed to be proportional to stagger angle while downstream shows an opposite phenomenon. However, the effect of stagger angle on the downstream spectrum is generally small, particularly at high frequencies.

(a)
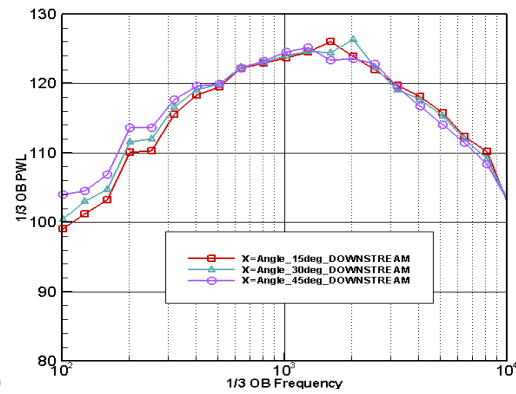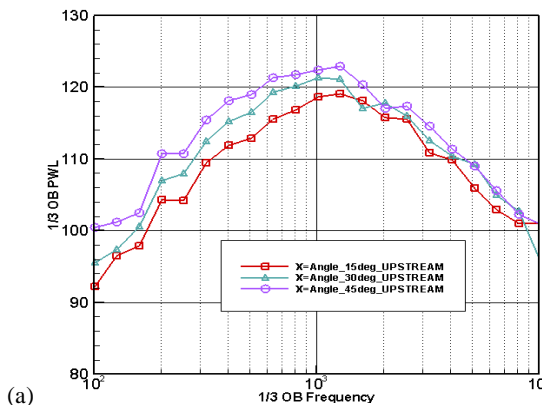
(b)

Figure 6. Variation of acoustic power spectrum with stagger angle, θ. (a) upstream and (b) downstream.

Figure 7 shows the power spectrum for the Mach number of 0.4, 0.5 and 0.6. At the high frequency range, the acoustic power both upstream and downstream is observed to increase with Mach number, of which the reason is attributed mainly to the convection effect, as given in Eq. (20).

(a)
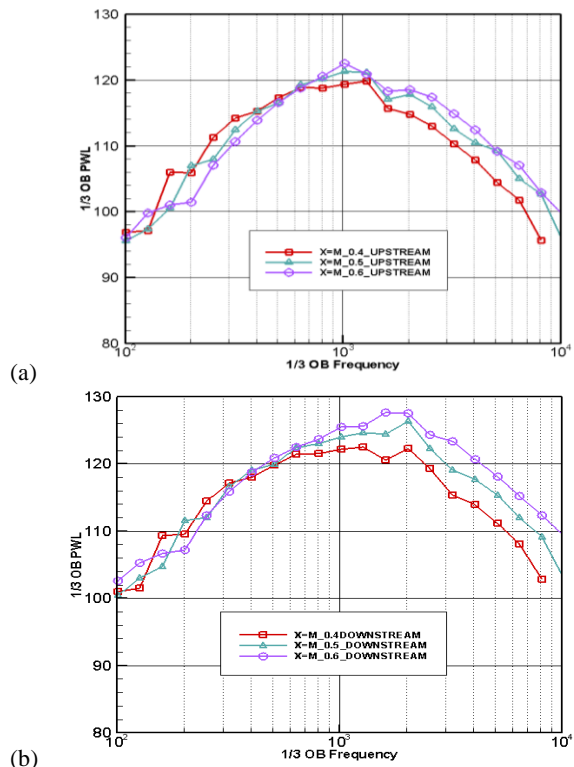
(b)

Figure 7. Variation of acoustic power spectrum with Mach number, M. (a) upstream and (b) downstream.

Figure 8 shows the power spectrum for the gap-chord ratio $s/c = 0.4, 0.8$ and 1.2. As the approximate expression of Eq. (42) in Ref. [7] predicts that the sound power is independent of gap-chord ratio (or solidity) above the critical frequency, chord length has little effect on sound radiation. However, at the high frequency range, as gap-chord ratio increases, the acoustic power both upstream and downstream is observed to slightly decrease.

(a)

(b)
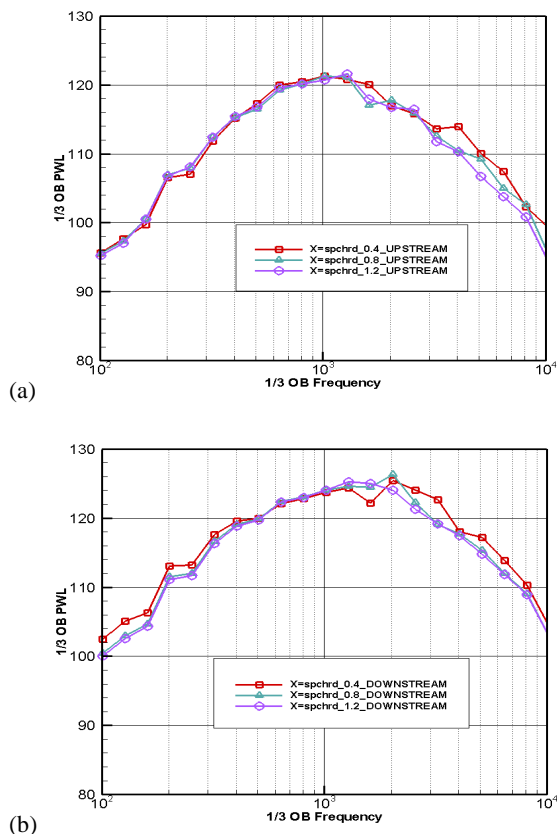
Figure 8. Variation of acoustic power spectrum with gap-chord ratio, s/c. (a) upstream and (b) downstream.

A similar parametric study is carried by Cheong et al. [7] under the same condition. The trends with various parameters obtained here closely match those obtained by Cheong et al. [7] which used two-dimensional theory, especially at high frequencies. The reason for this can be explained by the descriptions given in Section III.

CONCLUSION

Characteristics of the acoustic power spectrum, upstream and downstream of a three-dimensional cascade of flat plates bounded by two parallel walls impinging by isotropic frozen turbulent gusts have been investigated. The acoustic power spectrum formulation was derived, which includes the effects of span-wise wavenumber components of the impinging turbulent gust. This three-dimensional theory is based on the previous tonal noise theory of Smith [2] and its generalization to two-dimensional broadband noise theory by Cheong et al [7]. The validity of the present model is confirmed by comparing its prediction with the experiment.

Through the comparison of the acoustic power spectra predicted using the present three-dimensional model with those using the two-dimensional formula by Cheong et al. [7, 8], it is shown that the variation of the spectra with the frequencies comes to closer agreement between two prediction as the frequency increases, whereas there is significant difference of increasing rate of the spectra at lower frequencies. These results can be understood by noting the different dispersion relations between two- and three- dimensional acoustic fields. However, the closer agreements between the two models at higher frequencies allow the main findings provided in the previous works [7, 8] based on two-dimensional model to be valid and applied for the three dimensional broadband noise due to the interaction of the ingesting turbulence with the rectilinear cascade of flat plates bounded by two side walls.

Through the subsequent parameter study, we aim at finding out the effect of different parameters such as stagger angle and blade number on the whole acoustic power. As discussed in the parametric study section, with Mach number and blade number increases, the acoustic power both upstream and downstream increases; with stagger angle increases, the acoustic power upstream decreases while the downstream acoustic power increases; and with gap-chord ratio increases, the acoustic power spectrum both upstream and downstream does not show significant differences. This can be utilized as the reference when designing the aero-engine fan.

ACKNOWLEDGEMENT

REFERENCES

1 T.F.Brooks, D.S.Pope, and M.A.Marcolini, "Airfoil self-noise and prediction", NASA RP1218, 1989

2 S.N.Smith, "Discrete frequency sound generation in axial flow turbomachines", Reports and Memoranda No.3709, Aeronautical Research Control Council, London, 1972

3 D.S.Whitehead, "Classical two-dimensional methods", in Unsteady Turbomachinery Aerodynamics (AGARD-AG-298), edited by M.F.Platzer and F.O.Carta, AGARD Manual on Aeroelasticity in Axial Flow Turbomachines, Vol.1 (Neuilly sur Seine, France, 1987),Chap.3

4 S.A.L.Glegg, "The response of a swept blade row to a three-dimensional gust", J.Sound Vib. 227, 29-64

5 D.B.Hanson and K.P.Horan, "Turbulence/cascade interaction: Spectra of inflow, cascade response, and noise", AIAA-98-2319, 1998

6 D.B.Hanson, "Influence of lean and sweep on noise of rotor and stator cascade with inhomogeneous inflow turbulence including effects of lean and sweep", NASA Contract Rep. NASA CR 2001-210762

7 C. Cheong, P. Joseph, and S. Lee, "High frequency formulation for the acoustic power spectrum due to cascade-turbulence interaction", Journal of the Acoustical Society of America 119 (2006), no.1, 108-22

8 C.Cheong, V.Jurdic, and P.Joseph, "Decomposition of modal acoustic power due to cascade-turbulence interaction", JSV,Vol.324, No.1-2, pp.57-73, 2009

9 R.K.Amiet, "Acoustic radiation from an airfoil in a turbulent stream",J.Sound Vib. no.4, 407-420(1975)

10 M.E.Goldstein, Aeroacoustics, McGraw-Hill, New York, 1976.